Atomic exchange correction in forbidden unique beta transitions

Xavier Mougeot

Atomic exchange correction in forbidden unique beta transitions

Xavier Mougeot [a, 1]

[a] Université Paris-Saclay, CEA, List, Laboratoire National Henri Becquerel (LNE-LNHB), 91120, Palaiseau, France

Abstract

The theoretical modelling of the atomic exchange effect, until now only available for allowed beta decays, has been extended to the forbidden unique transitions. The required computing power for such calculations being important, an extensive tabulation of the correction factors has been conducted. These tables will be included in the future version of the BetaShape code, which atomic screening has also been revised to ensure the same level of accuracy as for exchange. Results for several radionuclides are discussed.

Keywords: Beta spectra, atomic effects, exchange, screening, forbidden transition, BetaShape.

1. Introduction

The Extended International Reference System (ESIR) is being developed by the International Bureau of Weights and Measures (BIPM) (Coulon, 2022). The objective is to create a specific instrument for comparing primary standards of radionuclides decaying almost purely through alpha, beta and low-energy electron capture transitions, for which gamma emission is non-existent or extremely low. The measuring device is based on the liquid scintillation counting technique with the triple-to-double coincidence ratio (TDCR) method and

[1] Corresponding author: xavier.mougeot@cea.fr

a 0.1% standard uncertainty is aimed at (Coulon, 2021). CIEMAT/NIST is the other standard method commonly employed in radionuclide metrology when carrying out liquid scintillation activity measurements. In the case of beta decaying radionuclides, both methods necessitate precise knowledge of the energy spectrum of the emitted beta particles to compute the detection efficiency (Broda, 2007).

Recent studies (Kossert, 2015; Kossert, 2018; Kossert, 2021) have demonstrated that not using an accurate description of the very low-energy part of the spectrum, where atomic effects play a major role, can lead to an underestimation of the activity of a fraction of a percent, and even more than a percent in some cases. In addition, observed discrepancies between the activities determined with these two methods are resolved when using accurate theoretical modelling for the calculation of beta spectra.

In this context, two atomic phenomena are important. The first one is the well-known screening effect, i.e. how the atomic electrons screened the Coulomb potential of the nucleus feels by the ejected beta particle. The second one is the exchange effect, a pure quantum phenomenon that comes from the indistinguishability of the electrons. The direct decay creates an electron in a continuum state. The exchange effect adds another decay channel, thus increasing the total transition probability, by allowing a beta particle to be created into a bound orbital of the parent atom, with the simultaneous ejection of the atomic electron into the continuum. Consequently, such an effect cannot occur in beta plus transitions and is thus specific to beta minus decays.

We have continuously developed for many years a specific code called BetaShape which aims at providing improved theoretical predictions of beta decays (Mougeot, 2017) and electron captures (Mougeot, 2018; Mougeot, 2019). The current released version[2] (2.2) includes radiative corrections based on the work of Towner and Hardy (2008) on superallowed

[2] Available at: http://www.lnhb.fr/rd-activities/spectrum-processing-software/

transitions, which were found in (Turkat, 2023) to be in excellent agreement with their latest predictions given in (Hardy, 2020). Version 2.2 also includes an analytical screening correction that gives good results above a few keV, but which is too imprecise at very low energy for an accurate description of the beta spectrum. Moreover, the exchange effect is not included in the BetaShape modelling.

We started our first study of the atomic exchange effect years ago (Mougeot, 2012; Mougeot, 2014) using the formalism of Harston and Pyper (1992). However, they restricted their description to allowed transitions only, for which the angular momentum carried away by the beta particles limits the exchange process to atomic electrons in $s_{1/2}$ and $p_{1/2}$ orbitals. In (Kossert, 2021), we assumed that this exchange correction could be applied as an estimate to the forbidden unique transitions involved in ^{90}Sr/^{90}Y decays. Correctness of such an approximation is simply questionable.

The purpose of the present work is therefore to establish a modelling of the atomic exchange correction extended to forbidden beta transitions. The beta particles can then be emitted with higher angular momenta and exchange becomes possible with atomic electrons in other orbitals. We focus this study on the forbidden unique transitions because they do not necessitate any input information from nuclear structure, contrary to forbidden non-unique decays. The correction associated to a specific angular momentum is found to act on the corresponding component with identical angular momentum in the shape factor. Consequently, overlaps of continuum and bound relativistic electron wave functions have to be calculated for all the possible angular momenta at each beta particle kinetic energy.

We first describe in Section 2 our extended modelling of the exchange effect. Such calculations require a lot of computing power for any beta spectrum. In addition, a screening correction determined from a full numerical solution of the Dirac equation is needed, which represents also a heavy computational load. Section 3 summarizes our efforts to make available

these two atomic corrections in the next released version of BetaShape ensuring good accuracy. Finally, theoretical predictions for some transitions of interest are presented in Section 4.

2. Theoretical formalism

Pyper and Harston (1988) studied in detail the atomic effects that are theoretically expected to influence the beta decays. In particular, their formalism includes a derivation of the atomic exchange effect, but simplified to the allowed transitions. The purpose of the present work is to establish a formulation of the atomic exchange effect extended to the forbidden unique transitions, consistent with the reference formalism of beta decays from Behrens and Bühring (1982).

Following the methodology in (Pyper, 1988), we start from the expression of the transition matrix without atomic states, given in Chapter 6 in (Behrens, 1982).

$$T_{\beta^-} = \frac{G_\beta}{\sqrt{2}}\frac{1}{\pi^{3/2}}\sum_{KLsM}\sum_{\substack{\kappa_e\mu_e\\ \kappa_\nu\mu_\nu}}(-1)^{J_f-M_f+j_e-\mu_e}(-1)^{L+M+j_\nu+\mu_\nu}\sqrt{2J_i+1}\begin{pmatrix} J_f & K & J_i \\ -M_f & M & M_i\end{pmatrix}$$

$$\times\begin{pmatrix} j_e & K & j_\nu \\ -\mu_e & -M & -\mu_\nu\end{pmatrix}a^*_{\kappa_e\mu_e}b^*_{\kappa_\nu\mu_\nu}\int_0^\infty q^2\mathrm{d}q\int_0^\infty r^2\mathrm{d}r\,\frac{(qR)^L}{(2L+1)!!}j_L(qr)F_{KLs}(q^2)$$

$$\times\left\langle\phi'_{\kappa_e}\|T_{KLs}(1+\gamma_5)\|\phi_{\kappa_\nu}\right\rangle \qquad (1)$$

It results from a double multipole expansion: on the one hand of the nuclear current (K, L, s, M); on the other hand of the lepton current $(\kappa_e, \mu_e, \kappa_\nu, \mu_\nu)$, with κ the angular momentum quantum number and μ the orbital magnetic quantum number. We refer the reader to (Behrens, 1982) for the definition of all the quantities. The decay is described as a one-body transition, i.e. from an initial neutron in the parent nucleus to a final proton in the daughter nucleus. Applying the Wigner-Eckart theorem on the corresponding spherical one-body tensor operator $T_{KLs}(1+\gamma_5)$ allows to split the radial and angular parts. The latter is developed on a basis of angular momentum eigenstates, which makes Clebsch-Gordan coefficients (or 3*j*-symbols) appear.

Combining the angular momenta and spins of the four particles involved in the decay (neutron, proton, electron and antineutrino) creates 6*j*-symbols, visible in Equation (1), and 9*j*-symbols that are hidden in the reduced matrix elements $F_{KLs}(q^2)$ (nuclear) and $\langle \phi'_{\kappa_e} \| T_{KLs}(1+\gamma_5) \| \phi_{\kappa_\nu} \rangle$ (lepton). The product of these reduced matrix elements is integrated over the entire space (on the radial part *r*) and over the momentum *q* transferred in the decay.

In such description of the process, the initial and final atomic electrons are assumed identical. However, the weak interaction changes the nucleus charge and the decay occurs is in reality between initial and final atomic states that are not orthogonal. It is thus necessary to revise the initial and final lepton states in Equation (1) by including the atomic wave functions.

The global atomic wave function can be described following the same logic in terms of angular and radial components. An orthonormal, complete basis of one-particle wave functions is defined, for which the radial part is separated thanks to the introduction of spin-orbital functions (Lödwin, 1955). The degeneracy of each spin-orbital function is given by its relative occupation number, i.e. the average number of electrons in the considered one-particle state. The global atomic wave function is then expressed in configuration space and must be antisymmetric. Considering an ordered configuration, this wave function is a Slater determinant of the one-particle wave functions.

The reduced lepton matrix element $\langle \phi'_{\kappa_e} \| T_{KLs}(1+\gamma_5) \| \phi_{\kappa_\nu} \rangle$ has to be modified by evaluating the operator between two states that include the atomic electrons and the leptons created in the decay. Lödwin established in (Lödwin, 1955) the very general formula of the transition matrix between two non-orthogonal states expressed by Slater determinants. The Hermitian operator is considered in its very general nature and expanded as a sum of many-particle operators (zero-, one-, two-, etc.). In the present study, we stay with the assumption of a process described in Equation (1) by a one-particle operator. We end up with evaluating a

single determinant that contains many overlaps in the off-diagonal terms between initial $|\phi_i\rangle$ and final $|\phi'_j\rangle$ atomic one-particle wave functions.

$$T_{\beta^-} = \frac{G_\beta}{\sqrt{2}}\frac{1}{\pi^{3/2}}\sum_{KLsM}\sum_{\substack{\kappa_e\mu_e\\ \kappa_\nu\mu_\nu}}(-1)^{J_f-M_f+j_e-\mu_e}(-1)^{L+M+j_\nu+\mu_\nu}\sqrt{2J_i+1}\begin{pmatrix} J_f & K & J_i \\ -M_f & M & M_i\end{pmatrix}$$

$$\times\begin{pmatrix} j_e & K & j_\nu \\ -\mu_e & -M & -\mu_\nu\end{pmatrix}a^*_{\kappa_e\mu_e}b^*_{\kappa_\nu\mu_\nu}\int_0^\infty q^2\mathrm{d}q\int_0^\infty r^2\mathrm{d}r\,\frac{(qR)^L}{(2L+1)!!}j_L(qr)F_{KLs}(q^2)$$

$$\times\begin{vmatrix} \langle\phi'_1|\phi_1\rangle & \langle\phi'_1|\phi_2\rangle & \cdots & \langle\phi'_1|\phi_N\rangle & \langle\phi'_1\|T_{KLs}(1+\gamma_5)\|\phi_{\kappa_\nu}\rangle \\ \langle\phi'_2|\phi_1\rangle & \langle\phi'_2|\phi_2\rangle & \cdots & \langle\phi'_2|\phi_N\rangle & \langle\phi'_2\|T_{KLs}(1+\gamma_5)\|\phi_{\kappa_\nu}\rangle \\ \vdots & \vdots & \ddots & \vdots & \vdots \\ \langle\phi'_N|\phi_1\rangle & \langle\phi'_N|\phi_2\rangle & \cdots & \langle\phi'_N|\phi_N\rangle & \langle\phi'_N\|T_{KLs}(1+\gamma_5)\|\phi_{\kappa_\nu}\rangle \\ \langle\phi'_{\kappa_e}|\phi_1\rangle & \langle\phi'_{\kappa_e}|\phi_2\rangle & \cdots & \langle\phi'_{\kappa_e}|\phi_N\rangle & \langle\phi'_{\kappa_e}\|T_{KLs}(1+\gamma_5)\|\phi_{\kappa_\nu}\rangle \end{vmatrix} \quad (2)$$

The nuclear charge differing only by one proton, these off-diagonal overlaps can be neglected, i.e. $\forall(i,j), i\neq j, \langle\phi'_j|\phi_i\rangle \approx 0$, which corresponds to neglecting the shake-up and shake-off processes in the decay. The latter determinant is then established straightforwardly with the lower-upper decomposition method.

$$\begin{vmatrix} \langle\phi'_1|\phi_1\rangle & 0 & \cdots & 0 & \langle\phi'_1\|T_{KLs}(1+\gamma_5)\|\phi_{\kappa_\nu}\rangle \\ 0 & \langle\phi'_2|\phi_2\rangle & \cdots & 0 & \langle\phi'_2\|T_{KLs}(1+\gamma_5)\|\phi_{\kappa_\nu}\rangle \\ \vdots & \vdots & \ddots & \vdots & \vdots \\ 0 & 0 & \cdots & \langle\phi'_N|\phi_N\rangle & \langle\phi'_N\|T_{KLs}(1+\gamma_5)\|\phi_{\kappa_\nu}\rangle \\ \langle\phi'_{\kappa_e}|\phi_1\rangle & \langle\phi'_{\kappa_e}|\phi_2\rangle & \cdots & \langle\phi'_{\kappa_e}|\phi_N\rangle & \langle\phi'_{\kappa_e}\|T_{KLs}(1+\gamma_5)\|\phi_{\kappa_\nu}\rangle \end{vmatrix} = \left[\prod_{i=1}^N\langle\phi'_i|\phi_i\rangle\right]\times$$

$$\left[\langle\phi'_{\kappa_e}\|T_{KLs}(1+\gamma_5)\|\phi_{\kappa_\nu}\rangle - \sum_{i=1}^N\langle\phi'_i\|T_{KLs}(1+\gamma_5)\|\phi_{\kappa_\nu}\rangle\frac{\langle\phi'_{\kappa_e}|\phi_i\rangle}{\langle\phi'_i|\phi_i\rangle}\right] \quad (3)$$

The transition probability is essentially determined by the square of the transition matrix. It depends on the directions of the emitted leptons, but also on each of the magnetic quantum numbers of the particles involved in the initial and final states. Focusing on the beta spectrum as the observable of interest, one has to integrate over all the possible, undetected directions of the leptons. In addition, no orientation of the initial and final nuclear states is observed, which means that the beta spectrum does not depend on the magnetic substates. We have therefore to

average over these initial substates and to sum over these final substates. Without considering the atomic states, the transition probability of the beta particle with an energy W is given by (Behrens, 1982)

$$P(W) = \frac{G_\beta^2}{2\pi^3} pW {p_\nu}^2 F_0 L_0 C(W) \tag{4}$$

with $p = \sqrt{W^2 - 1}$ the electron momentum, $p_\nu = (W_0 - W)$ the antineutrino momentum, W_0 the transition energy and $F_0 L_0$ the Fermi function defined from the Coulomb amplitude $\alpha_{\pm 1}$ of the relativistic electron wave functions

$$F_0 L_0 = \frac{\alpha_{-1}^2 + \alpha_{+1}^2}{2p^2} \tag{5}$$

The Coulomb amplitudes are actually labelled with κ_e, which can take positive or negative integer values. A convenient notation to introduce is $k = |\kappa_e|$. The shape factor $C(W)$ in its usual form is given for allowed and forbidden unique transitions by

$$C(W) = \left\{ \left[{}^V F_{000}^{(0)} \right]^2 \delta_{L,1} + \left[{}^A F_{L,L-1,1}^{(0)} \right]^2 \right\} \frac{R^{2(L-1)}}{[(2L-1)!!]^2} (2L-1)! \sum_{k=1}^{L} \lambda_k \frac{p^{2(k-1)} {p_\nu}^{2(L-k)}}{(2k-1)![2(L-k)+1]!} \tag{6}$$

The first two terms of the right-hand side are the dominant form factor coefficients $F_{KLs}(q^2)$ involved in the decay, and are either of vector (V) or axial-vector (A) type. R is nuclear radius. For an allowed transition, $L = 1$ and $\lambda_1 = 1$. If $L > 1$, the transition is $(L-1)^{\text{th}}$ forbidden unique.

Deriving the shape factor over again, we use the transition matrix with the atomic states and establish a corrected shape factor.

$$C(W) = \left\{ \left[{}^V F_{000}^{(0)} \right]^2 \delta_{L,1} + \left[{}^A F_{L,L-1,1}^{(0)} \right]^2 \right\} \frac{R^{2(L-1)}}{[(2L-1)!!]^2} (2L-1)! \, C_{\text{ov}} \sum_{k=1}^{L} \lambda_k \frac{p^{2(k-1)} {p_\nu}^{2(L-k)}}{(2k-1)![2(L-k)+1]!} \times$$

$$[1 + \eta_{-k} + \eta_{+k}] \tag{7}$$

As in our previous study of electron capture (Mougeot, 2018; Mougeot, 2019), we now labels the atomic states with their quantum numbers (n, κ). The Coulomb amplitudes of their wave

functions is denoted by $\beta_{n\kappa}$, their relative occupation number by $n_{n\kappa}$ and their momentum by $p_{n\kappa}$. The overlap term that appears in Equation (7) is given by

$$C_{\mathrm{ov}} = \sum_{(n,\kappa)} \langle \phi'_{n\kappa} | \phi_{n\kappa} \rangle^{2|\kappa| n_{n\kappa}} \tag{8}$$

and only acts as a constant factor, without changing the spectrum shape. Each beta electron created in a $\pm k$ state sees its probability modified by an exchange correction due to the atomic electrons of the same $\pm k$ angular momentum. This correction corresponds to the latest term of Equation (7) and is expressed as

$$\eta_\kappa = \frac{T_\kappa^2 - 2\alpha_\kappa T_\kappa}{\alpha_{-k}^2 + \alpha_{+k}^2} \tag{9}$$

with

$$T_\kappa = \sum_{(n,\kappa)} \sqrt{n'_{n\kappa}} \frac{\langle \phi'_{C,\kappa} | \phi_{n\kappa} \rangle}{\langle \phi'_{n\kappa} | \phi_{n\kappa} \rangle} \beta'_{n\kappa} \left[\frac{p'_{n\kappa}}{p} \right]^{k-1} \tag{10}$$

where the final electron continuum state $|\phi'_{\kappa_e}\rangle$ has been relabelled as $|\phi'_{C,\kappa}\rangle$ for better clarity.

This formulation of the atomic exchange effect is consistent with the result of Pyper (1988) and Harston (1992) for the allowed transitions if, as them, we assume closed shells and perfect overlap of the atomic wave functions, i.e. $\forall i, \langle \phi'_i | \phi_i \rangle \approx 1$.

To illustrate how the exchange correction acts, we now consider the case of a first forbidden unique transition. Its usual shape factor is given by

$$C(W) = {p_\nu}^2 + \lambda_2 p^2 \tag{11}$$

The first term is associated to $k = 1$ states and the second to $k = 2$ states. The exchange correction is thus applied as

$$C(W) = {p_\nu}^2 \times [1 + \eta_{-1} + \eta_{+1}] + \lambda_2 p^2 \times [1 + \eta_{-2} + \eta_{+2}] \tag{12}$$

In any atom, the number of $s_{1/2}$ ($\kappa = -1$) and $p_{1/2}$ ($\kappa = +1$) orbitals is higher and they are most often closed. Their contribution is therefore naturally higher. In addition, the overlap with the continuum states is higher than for other κ value. The ratio of momenta in Equation (10) acts in the same direction. Finally, in any forbidden unique shape factor the p_ν term dominates

at low energy, where the exchange effect is the most significant. With this analysis, we conclude that applying the allowed exchange correction simply to the Fermi function, neglecting its influence on the shape factor, is a good approximation for the forbidden unique transitions.

3. Embedment in BetaShape

The computational burden to determine the exchange correction is significant, typically several tens of minutes on a recent 16-processor workstation for a single beta spectrum with fine energy binning. In order to make these predictions available in a simple manner through the BetaShape code, extensive tabulation of the exchange correction factors $[1 + \eta_{-k} + \eta_{+k}]$ has been considered. The atomic wave functions used for the electron capture calculations (Mougeot, 2018; Mougeot, 2019) have been employed.

However, the atomic screening correction in BetaShape had also to be revised because the analytical correction in the released version 2.2 is not as accurate as the exchange correction. It is based on an analytical approach developedby Bühring (1984) in which the wave function of the beta particle, established from a simplified version of the coupled Dirac equations, is expanded radially together with a screened potential. Keeping only the dominant term, Bühring established formulas that estimate screened-to-unscreened ratios for the Fermi function $F_0 L_0$ and the λ_k parameters. This correction was adapted in previous work with more precise screened potentials (Mougeot, 2016). In the present study, full numerical computation of the screening effect on the Fermi function and on the λ_k parameters that enter in the definition of the shape factors has been performed. Screened-to-unscreened ratios have been extensively tabulated.

For both atomic corrections, tables have been generated for all elements up to $Z = 120$. An energy grid with non-constant spacing has been considered in order to ensure sufficient precision at very low energy: with a total of 500 points up to 30 MeV, 220 of them are below

100 keV and 80 from 1 eV to 5 keV. For the exchange effect, all atomic orbitals have been considered and a numerical precision of at least 0.001% has been ensured, i.e. the tabulation ends when all the exchange correction factors of a given element are less than 1.00001. Beyond the last tabulated energy, exchange correction factors are assumed equal to unity. For the screening effect, considered for both beta plus and beta minus decays, the Fermi function and the λ_k parameters have been tabulated up to 30 MeV and λ_7, which corresponds to a sixth forbidden unique transition and covers more than the known transitions. Interpolation within these tables allows the fast and precise inclusion of these atomic effects in the beta spectra provided by the BetaShape code. They will be included in the future released version 2.3.

4. Results

We first apply the present modelling to the allowed low-energy transition of ^{63}Ni decay. The spectrum predicted with the version 2.2 of BetaShape (green) is compared in Figure 1 to the spectrum calculated with the tabulated screening correction (red). The improvement on the shape at very low energy, below 1 keV, is clearly visible. The spectrum that also includes the tabulated exchange correction (blue) and a precise measurement (black) performed with a Metallic Magnetic Calorimeter (MMC) (Loidl, 2014) are given too. The calculated spectra are only normalized to the measured spectrum with a global constant factor. The present modelling describes very well the experimental spectrum over the entire energy range, down to the energy threshold below 0.5 keV.

The same comparison is shown in Figure 2 in the case of ^{241}Pu decay. This first forbidden non-unique transition can be treated as allowed with the ξ-approximation (Mougeot, 2015). The measurement was also performed with an MMC (Loidl, 2010), and conclusion is the same as for ^{63}Ni decay.

Testing the theoretical predictions of the atomic exchange correction in the case of the forbidden unique transitions is made difficult by the inexistence of precise measurement down to low energy. An indirect validation was done recently in the context of dark matter studies. In such experiments, the accuracy of the background modelling is pivotal and some naturally occurring radionuclides still contribute, despite all the significant efforts to reduce their amount. The DarkSide experiment is based on a dual-phase liquid argon time projection chamber that makes it sensitive to the ^{37}Ar and ^{39}Ar decays (Agnes, 2021). The latter is a pure first forbidden unique beta transition. The experiment is also sensitive to the ^{85}Kr decay, which exhibits an almost pure transition of the same nature. Figures 3 and 4 present the different predictions for ^{39}Ar and ^{85}Kr beta spectra. The probability increase at low energy was demonstrated to be one of the important ingredient to significantly improve the background description (Agnes1, 2023), setting new limits on some dark matter particle interactions (Agnes2, 2023; Agnes3, 2023).

Another possibility is to apply the correction factors to forbidden non-unique transitions. Equations (7) and (12) show that the atomic exchange correction acts on the λ_k parameters in forbidden unique transitions. These parameters are still present in the theoretical shape factor of forbidden non-unique transitions, within each multipole of the currents expansion. We can thus consider a "forbidden unique approximation" of the atomic exchange effect by applying the correction factors in the same manner. This was done recently for the studies of ^{151}Sm (Kossert, 2022) and ^{176}Lu (Quarati, 2023) decays. In both cases, significant influence of nuclear structure was found down to the lowest energies, which prevents any firm conclusion. In ^{151}Sm decay, theory is not able to describe the strong probability increase below 4 keV, even if it is still not clear whether the discrepancy comes from theory or experiment. In ^{176}Lu decay, the beta spectrum of the dominant transition is well reproduced down to very low energy with residuals falling in $\pm 3\sigma$. The latter still exhibit a nonlinear trend that is most probably due to the description of the nuclear structure.

We want to emphasize that new high-precision measurements of forbidden beta transitions, both unique and non-unique, are required down the lowest energies. They would be of great help to test the different parts of the theoretical modelling and to quantify their accuracy. We suggest as a priority the measurement of the ^{107}Pd beta spectrum. This ground-state-to-ground-state decay is perfectly suitable for an MMC measurement and for testing the modelling: medium atomic number, first forbidden unique transition, half-life of 6.5(3) $\times 10^6$ y (Blachot, 2008) and Q-value of 34.0(23) keV (Wang, 2021). Figure 5 presents the different predictions for this decay, showing the expected influence of the atomic exchange effect.

5. Conclusion

Following their derivation done decades ago, we have extended the modelling of the atomic exchange effect from (Pyper, 1988), originally established only for the allowed transitions, to the forbidden unique decays. Assuming the same hypotheses, their formulation can be deduced from our modelling, which is fully consistent with the formalism of beta decays from (Behrens, 1982). Demonstration has been done that the allowed exchange correction applied to the Fermi function is a good approximation for the forbidden unique transitions. With a willing of dissemination, we have included these results in the BetaShape code thanks to an extensive tabulation of the correction factors. In order to ensure accurate predictions at very low energy, we also revised the screening effect in the BetaShape modelling, tabulating the correction factors on the Fermi function and the λ_k parameters. All these tables cover more than the known transitions and will be included in the forthcoming version of BetaShape.

We validated these developments with ^{63}Ni and ^{241}Pu beta decays, for which high-precision measurements performed with cryogenic detectors are available. Excellent agreement over the entire experimental energy range was obtained, from a few hundreds of eV to the Q-value. Facing the lack of precise measurement to compare with, we looked for an indirect validation

addressed in other studies published elsewhere. The spectra of ^{39}Ar and ^{85}Kr decays were calculated for the DarkSide collaboration, who show that the most accurate predictions lead to the best description of the background. We also applied the exchange correction factors in the calculation of ^{151}Sm and ^{176}Lu forbidden non-unique decays as an approximation. As expected, the dominant effect comes from nuclear structure and no firm conclusion can be drown about the exchange effect.

We propose ^{107}Pd decay as good candidate for a future high-precision measurement. Other forbidden transitions would also help to test the predictions, and to revise them if necessary. There is still room for new theoretical developments, and some are ongoing in the framework of the European project PrimA-LTD. For instance, the atomic modelling of BetaShape that generates the wave functions can be replaced by high-precision wave functions from modern approaches, e.g. Density Functional Theory or Multi-Configurational Dirac-Fock. Another improvement would be the complete calculation of the matrix elements in Equation (2), mixing nuclear, lepton and atomic wave functions, which is unavoidable for an accurate treatment of the forbidden non-unique transitions.

Acknowledgment

This work has received funding from the EMPIR project 20FUN04 PrimA-LTD, co-financed by the Participating States and from the European Union's Horizon 2020 research and innovation program.

References

Agnes, P., et al. (DarkSide Collaboration), 2021. Calibration of the liquid argon ionization response to low energy electronic and nuclear recoils with DarkSide-50. Physical Review D 104, 082005. doi: 10.1103/PhysRevD.104.082005

Agnes1, P., et al. (DarkSide Collaboration), 2023. Search for low-mass dark matter WIMPs with 12 ton-day exposure of DarkSide-50. Physical Review D 107, 063001. doi: 10.1103/PhysRevD.107.063001

Agnes2, P., et al. (DarkSide Collaboration), 2023. Search for Dark-Matter-Nucleon Interactions via Migdal Effect with DarkSide-50. Physical Review Letters 130, 101001 (2023). doi: 10.1103/PhysRevLett.130.101001

Agnes3, P., et al. (DarkSide Collaboration), 2023. Search for Dark Matter Particle Interactions with Electron Final States with DarkSide-50. Physical Review Letters 130, 101002. doi: 10.1103/PhysRevLett.130.101002

Behrens, H., Bühring, W., 1982. Electron Radial Wave Functions and Nuclear Beta Decay. Clarendon, Oxford.

Blachot, J., 2008. Nuclear Data Sheets for A = 107. Nuclear Data Sheets 109, 1383-1526. doi: 10.1016/j.nds.2008.05.001

Broda, R., Cassette, P., Kossert, K., 2007. Radionuclide metrology using liquid scintillation counting. Metrologia 44 (2007) S36-S52. doi: 10.1088/0026-1394/44/4/S06

Bühring, W., 1984. The screening correction to the Fermi function of nuclear β-decay and its model dependence. Nuclear Physics A 430, 1. doi: 10.1016/0375-9474(84)90190-8

Coulon, R., Judge, S., Liu, H., Michotte, C., 2021. The international reference system for pure beta-particle emitting radionuclides: an evaluation of the measurement uncertainties. Metrologia 58, 025007. doi: 10.1088/1681-7575/abe355

Coulon, R., et al, 2022. The new international reference system for pure α- and pure β-emitting radionuclides and some electron capture decaying radionuclides by liquid scintillation counting. Journal of Radioanalytical and Nuclear Chemistry 331, 3221-3230. doi: 10.1007/s10967-022-08337-7

Hardy, J.C., Towner, I.S., 2020. Superallowed $0^+ \rightarrow 0^+$ nuclear β decays: 2020 critical survey, with implications for V_{ud} and CKM unitarity. Physical Review C 102, 045501. doi: 10.1103/PhysRevC.102.045501

Harston M.R., Pyper N.C., 1992. Exchange effects in β decays of many-electron atoms. Physical Review A 45, 6282-6295. doi: 10.1103/PhysRevA.45.6282

Kossert, K., Mougeot, X., 2015. The importance of the beta spectrum calculation for accurate activity determination of ^{63}Ni by means of liquid scintillation counting. Applied Radiation and Isotopes 101, 40-43. doi: 10.1016/j.apradiso.2015.03.017

Kossert, K., Marganiec-Gałązka, J., Mougeot, X., Nähle, O.J., 2018. Activity determination of ^{60}Co and the importance of its beta spectrum. Applied Radiation and Isotopes 134, 212-218. doi: 10.1016/j.apradiso.2017.06.015

Kossert, K., Mougeot, X., 2021. Improved activity standardization of ^{90}Sr/^{90}Y by means of liquid scintillation counting. Applied Radiation and Isotopes 168, 109478. doi: 10.1016/j.apradiso.2020.109478

Kossert, K., et al., 2022. High precision measurement of the ^{151}Sm beta decay by means of a metallic magnetic calorimeter. Applied Radiation and Isotopes 185, 110237. doi: 10.1016/j.apradiso.2022.110237

Lödwin, P.O., 1955. Quantum Theory of Many-Particle Systems. I. Physical Interpretations by Means of Density Matrices, Natural Spin-Orbitals, and Convergence Problems in the Method of Configurational Interaction. Physical Review 97, 1474-1489. doi: 10.1103/PhysRev.97.1474

Loidl, M., et al., 2010. First measurement of the beta spectrum of ^{241}Pu with a cryogenic detector. Applied Radiation and Isotopes 68, 1454-1458. doi: 10.1016/j.apradiso.2009.11.054

Loidl, M., Rodrigues, M., Le-Bret, C., Mougeot, X., 2014. Beta spectrometry with metallic magnetic calorimeters. Applied Radiation and Isotopes 87, 302-305. doi: 10.1016/j.apradiso.2013.11.024

Mougeot, X., Bé, M.M., Bisch, C., Loidl, M., 2012. Evidence for the exchange effect in the β decay of ^{241}Pu. Physical Review A 86, 042506. doi: 10.1103/PhysRevA.86.042506

Mougeot, X., Bisch, C., 2014. Consistent calculation of the screening and exchange effects in allowed β^- transitions. Physical Review A 90, 012501. doi: 10.1103/PhysRevA.90.012501

Mougeot, X., 2015. Reliability of usual assumptions in the calculation of β and ν spectra. Physical Review C 91, 055504. doi: 10.1103/PhysRevC.91.055504

Mougeot, X., 2016. Systematic comparison of beta spectra calculations using improved analytical screening correction with experimental shape factors. Applied Radiation and Isotopes 109, 177-182. doi: 10.1016/j.apradiso.2015.11.030

Mougeot, X., 2017. BetaShape: A new code for improved analytical calculations of beta spectra. EPJ Web of Conferences 146, 12015. doi: 10.1051/epjconf/201714612015

Mougeot, X., 2018. Improved calculations of electron capture transitions for decay data and radionuclide metrology. Applied Radiation and Isotopes 134, 225-232. doi: 10.1016/j.apradiso.2017.07.027

Mougeot, X., 2019. Towards high-precision calculation of electron capture decays. Applied Radiation and Isotopes 154, 108884. doi: 10.1016/j.apradiso.2019.108884

Pyper N.C., Harston M.R., 1988. Atomic effects on β-decay. Proceedings of the Royal Society of London A 420, 277-321. doi: 10.1098/rspa.1988.0128

Quarati, F.G.A., et al., 2023. Measurements and computational analysis of the natural decay of ^{176}Lu. Physical Review C 107, 024313. doi: 10.1103/PhysRevC.107.024313

Towner, I.S., Hardy, J.C., 2008. Improved calculation of the isospin-symmetry-breaking corrections to superallowed Fermi β decay. Physical Review C 77, 025501. doi: 10.1103/PhysRevC.77.025501

Turkat, S., Mougeot, X., Singh, B., Zuber, K., 2023. Systematics of log ft values for β−, and EC/β+ transitions. Atomic Data and Nuclear Data Tables 152, 101584. doi: 10.1016/j.adt.2023.101584

Wang, M., Huang, W.J., Kondev, F.G., Audi, G., Naimi, S., 2021. The Ame2020 atomic mass evaluation. (II). Tables, graphs and references. Chinese Physics C 45, 030003. doi: 10.1088/1674-1137/abddaf

Highlights

- Atomic exchange is important for activity measurements of beta decaying nuclei.
- Existing theoretical model for allowed transitions is extended to forbidden unique.
- Atomic screening and exchange corrections are extensively tabulated.
- Future version of the BetaShape code will include these accurate corrections.
- Results for ^{39}Ar, ^{63}Ni, ^{85}Kr, ^{107}Pd and ^{241}Pu decays are discussed.

Figures

Figure 1 – Comparison of the ^{63}Ni spectrum measured by MMC (Loidl, 2014) with the calculation from BetaShape version 2.2 (Mougeot, 2017) and those of the new version from this work that includes the atomic screening and exchange effects (see Section 3). Version 2.2 only includes screening correction from (Bühring, 1984).

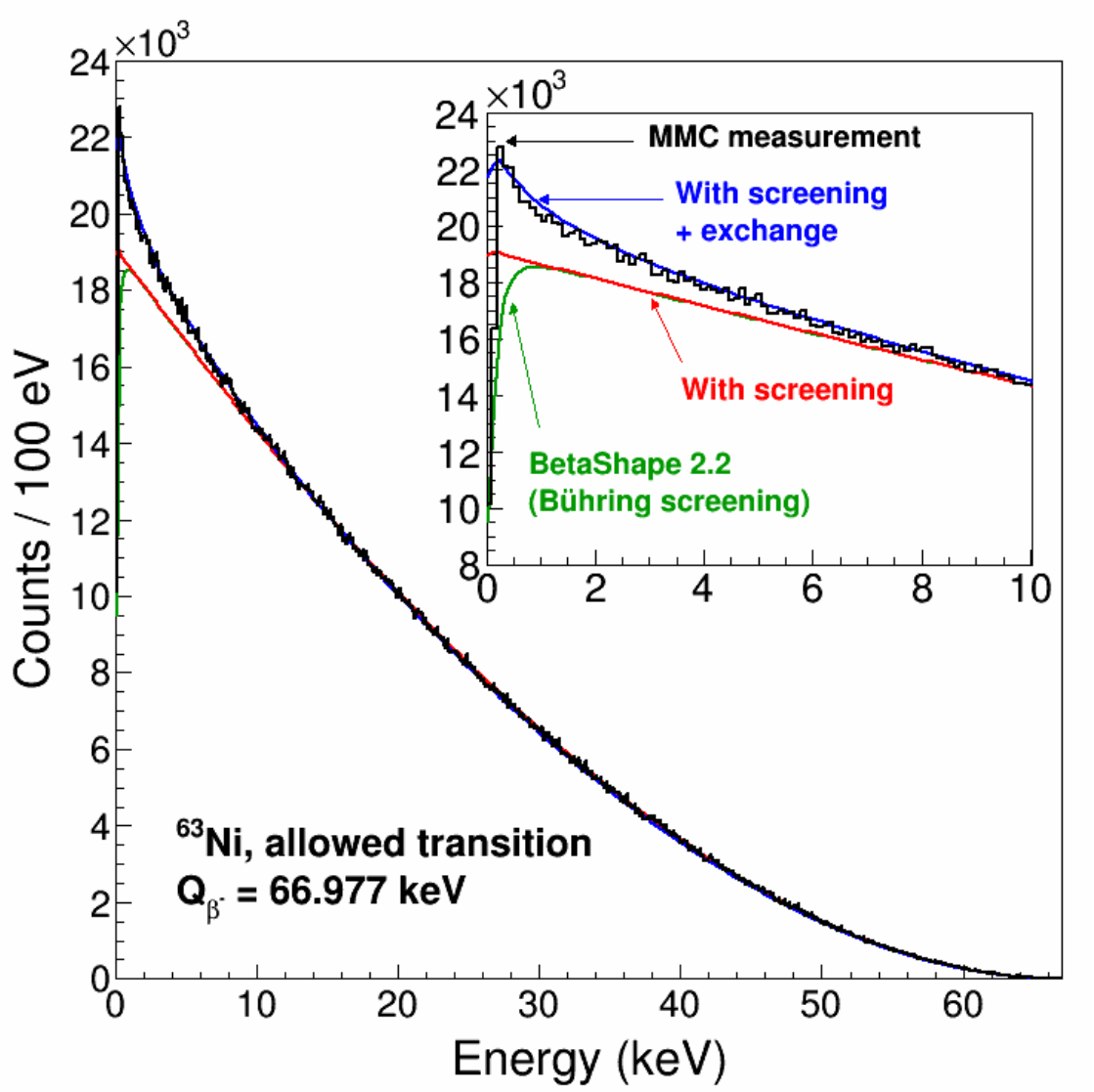
×10^3
Counts / 100 eV
Energy (keV)
63Ni, allowed transition
Q_β- = 66.977 keV
MMC measurement
With screening
+ exchange
With screening
BetaShape 2.2
(Bühring screening)

Figure 2 – Comparison of the ^{241}Pu spectrum measured by MMC (Loidl, 2010) with the calculation from BetaShape version 2.2 (Mougeot, 2017) and those of the new version from this work that includes the atomic screening and exchange effects (see Section 3). Version 2.2 only includes screening correction from (Bühring, 1984).

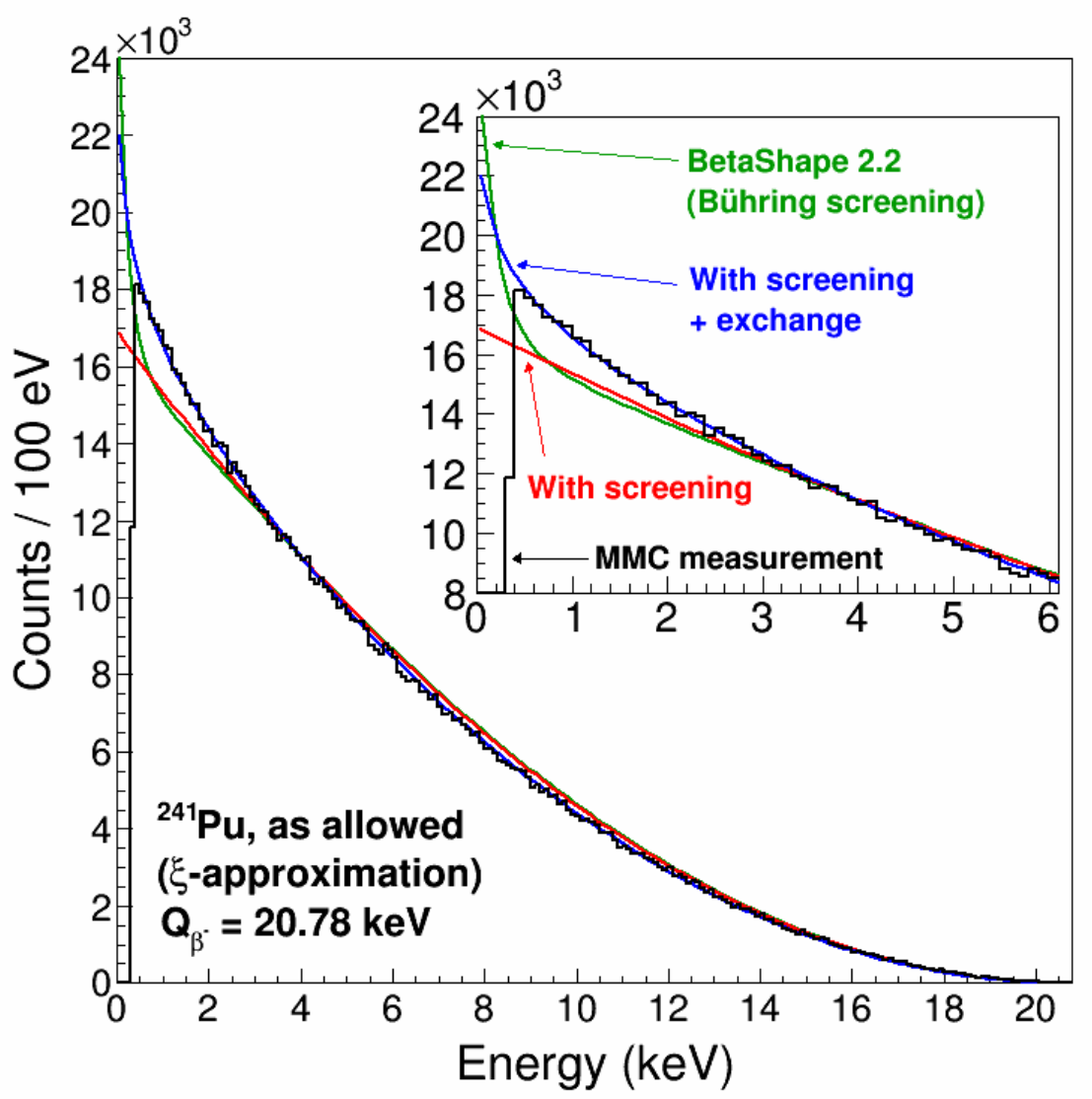

Figure 3 – Comparison of the ^{39}Ar spectrum calculated with BetaShape version 2.2 (Mougeot, 2017) with the predictions of the new version from this work that includes the atomic screening and exchange effects (see Section 3). Version 2.2 only includes screening correction from (Bühring, 1984).

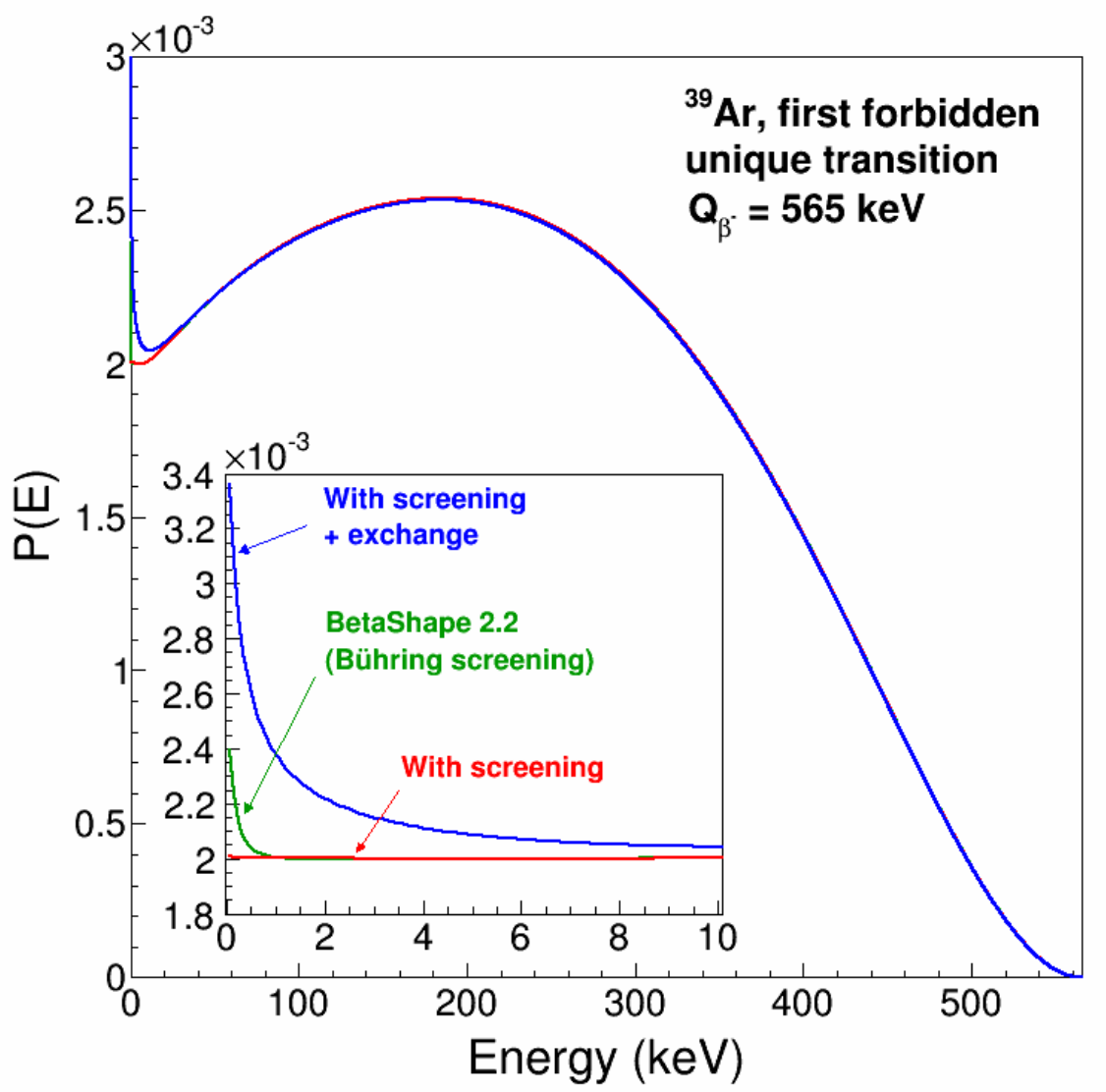

Figure 4 – Comparison of the ^{85}Kr spectrum calculated with BetaShape version 2.2 (Mougeot, 2017) with the predictions of the new version from this work that includes the atomic screening and exchange effects (see Section 3). Version 2.2 only includes screening correction from (Bühring, 1984).

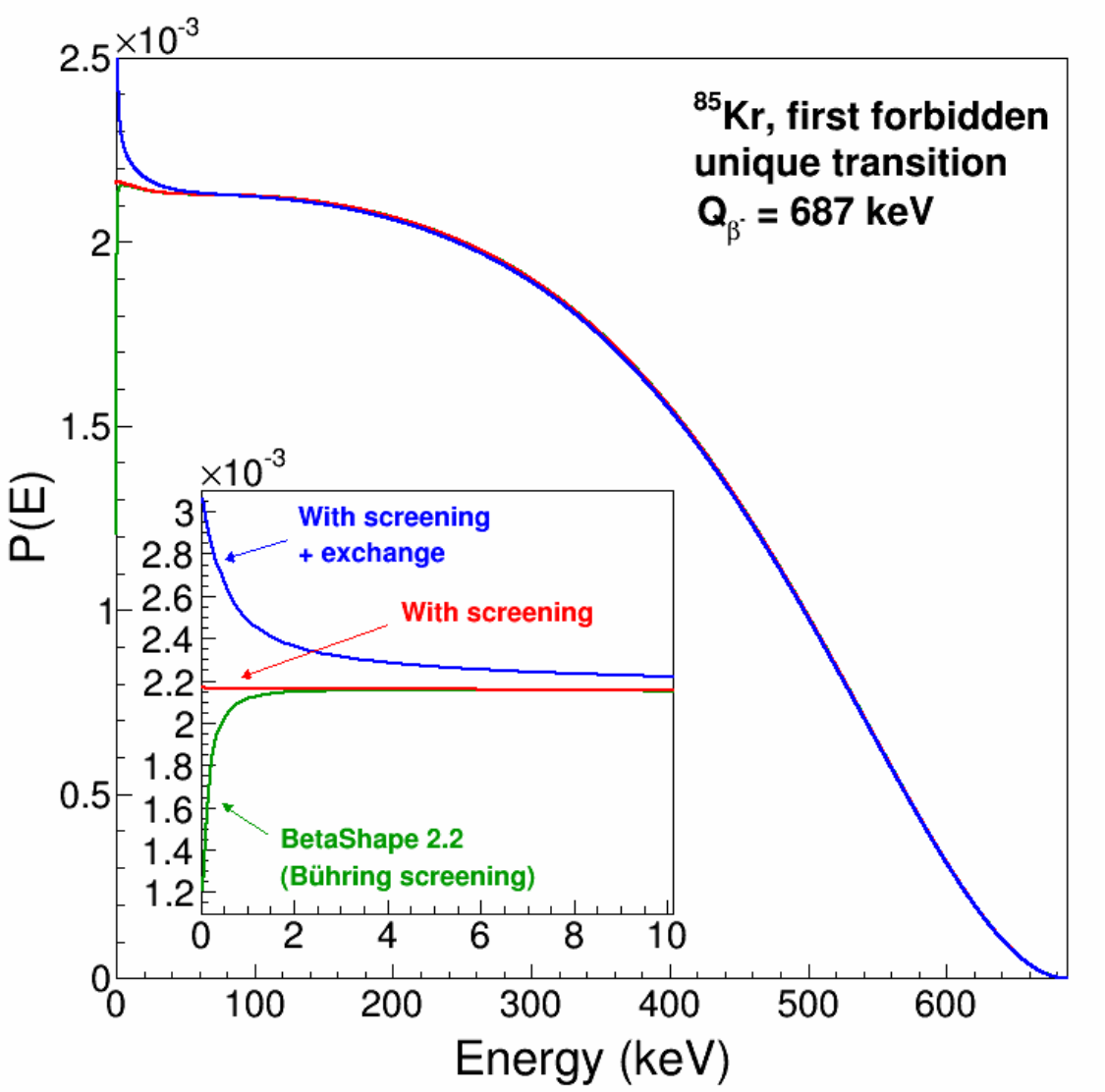

Figure 5 – Comparison of the ^{107}Pd spectrum calculated with BetaShape version 2.2 (Mougeot, 2017) with the predictions of the new version from this work that includes the atomic screening and exchange effects (see Section 3). Version 2.2 only includes screening correction from (Bühring, 1984).